PERGAMON

International Journal of Solids and Structures 39 (2002) 2031–2049

INTERNATIONAL JOURNAL OF SOLIDS and STRUCTURES

www.elsevier.com/locate/ijsolstr

Effect of a biasing electric field on the propagation of symmetric Lamb waves in piezoelectric plates

H. Liu [a], T.J. Wang [b], Z.K. Wang [b], Z.B. Kuang [a,*]

[a] *Department of Engineering Mechanics, Shanghai Jiaotong University, Shanghai 200240, China*
[b] *Department of Engineering Mechanics, Xi'an Jiaotong University, Xi'an 710049, China*

Received 21 August 2000; received in revised form 26 September 2001

Abstract

This paper is concerned with the effect of a biasing electric field on the propagation of Lamb waves in a piezoelectric plate. On the basis of three dimensional linear elastic equations and piezoelectric constitutive relations, the differential equations of motion under a biasing electric field are obtained and solved. Due to the symmetry of the plate, there are symmetric and antisymmetric modes with respect to the median plane of the piezoelectric plate. According to the characteristics of symmetric modes (odd potential state) and antisymmetric modes (even potential state), the phase velocity equations of symmetric and antisymmetric modes of Lamb wave propagation are obtained for both electrically open and shorted cases. The effect of a biasing electric field on the phase velocity, electromechanical coupling coefficient, stress field and mechanical displacement of symmetric and antisymmetric Lamb wave modes are discussed in this paper and an accompanying paper respectively. It is shown that the biasing electric field has significant effect on the phase velocity and electromechanical coupling coefficient, the time delay owning to the velocity change is useful for high voltage measurement and temperature compensation, the increase in the electromechanical coupling coefficient can be used to improve the efficiency of transduction.

Keywords: Biasing electric field; Symmetric Lamb waves; Phase velocity; Electromechanical coupling coefficient

1. Introduction

Lamb waves are elastic waves that propagate in plates of finite thickness. They have been widely used in physical, chemical and biological sensors (Wenzel and White, 1988), ultrasonic equipment for measuring mass density and viscosity of liquids (Wu and Zhu, 1996), flaw detection. Theoretical and the experimental investigations have demonstrated that there exist a variety of modes in the plate (Worlton, 1961; Toda, 1973; Shick et al., 1990), and the characteristics of each mode are determined by the ratio of plate thickness to wavelength. The waves can be divided into symmetric and antisymmetric modes, in which the zero-order symmetric mode (s_0) and antisymmetric mode (a_0) are the most useful ones (Wu and Zhu, 1996). The a_0

* Corresponding author.
E-mail address: zbkuang@mail.sjtu.edu.cn (Z.B. Kuang).

0020-7683/02/$ - see front matter
PII: S0020-7683(02)00014-8

mode is especially sensitive, fast in response, and can be adaptive to operate in liquid media (Joshi and Jin, 1991).

In recent years, there has been a growing interest in studying the effect of external perturbations such as biasing stresses, strains, pressure, temperature and electric fields on the propagation of acoustic waves. The main reasons for investigating the external perturbation effects are (Joshi, 1982): (1) to minimize the effect of certain variables on the propagation of the wave, (2) to utilize the effect to measure particular variable, e.g., application in SAW pressure sensors, SAW accelerometers, (3) to improve performance or select the most suitable operating conditions of SAW devices, e.g., selectivity of filters, stability of oscillators and temperature compensation of devices. The presence of a biasing state induced by external perturbations can significantly affect the characteristics of BAW and SAW. This fact is widely recognized and tackled by many investigators. For instance, Kessenikh and Shuvalov (1982) found that the application of a biasing electric field directed along the six or fourfold axis or a temperature-induced symmetry decrease at the phase transition can give rise to the existence of the transverse Bleustein–Gulyev surface wave. Sinha (1982) described the temperature and stress effects on the propagation of elastic waves in anisotropic solids by a perturbation procedure. Kuznetsova et al. (1998) presented theoretical results for the effects of differently oriented external electric field on the velocity of Bleustein–Gulyev surface acoustic waves in lithium niobate and strontium titanate for different mechanical crystal states, and revealed that the BG wave is unstable towards external effects. Sinha et al. (1985) considered the extensional and flexural deformations due to externally applied forces which have substantially effects on the change in the time delay, and demonstrated that such effects are strongly dependent on the type of loading, substrate geometry, orientation and propagation direction of surface waves. Dowaikh (1999) examined the propagation of Love waves in a pre-stressed layered half-space for an incompressible elastic material. Hussain and Ogden (2001) illustrated the influence of pure homogeneous strain on the reflection and transmission of plane waves at the boundary between two half-space of incompressible isotropic elastic material. Also, the influence of a biasing electric field on bulk waves, SAWs (Palmieri et al., 1986), Lamb waves (Palma et al., 1985a,b; Joshi, 1996) are experimentally investigated. Experiments have proved that SAW time-delay can be altered due to the biasing electric field, and this effect has great importance on improving the efficiency of SAW convolvers, the developments of high precision pressure sensors and stable resonate as well as nondestructive testing of structural material (Sinha, 1982). The use of acoustic wave propagation is particularly attractive due to the fact that lower voltages are needed to obtain the same electric intensity in comparison with bulk waves.

The interpretation of these effects can be given by the perturbation theory of small amplitude acoustic waves superposed on a bias (Tiersten, 1978). Based on this theory, the biasing field modifies the second order material constants, and the effective material constants which differ from those of the unbiased medium are described. In fact, when a static voltage is applied across the electrodes deposited on the surfaces of the plate, various components of mechanical stress and electric displacement are generated in the piezoelectric plate. These mechanical stresses and electric displacements can lead to a change in the velocity of the acoustic wave. The sensing principle of all the acoustic voltage sensors are based on the changes in acoustic wave velocity caused by an electric field. Due to the availability of large number of propagation modes and the wide choice of interaction conditions, Lamb waves in electric field controlled devices are especially attractive (Palma et al., 1985a,b). Lamb wave voltage sensors are highly stable, small, and sensitive to the applied voltage.

This contribution consists of two papers, in which we will present preliminary results of the change in phase velocity produced by a uniform biasing electric field on different Lamb wave modes propagating in the infinite piezoelectric plate. In the current paper we will concentrate on the symmetric Lamb waves. All the results are very useful for improving or varying performance of acoustic devices. Only linear piezoelectric effects are considered here. Further researches will be invoked to study the more complicated and important nonlinear piezoelectric effects and electrostriction.

2. Statement of the problem

2.1. Static electric field problem

The prototype geometry for a discussion of Lamb waves is shown in Fig. 1. The piezoelectric plate is symmetric about the media plane $z = 0$ and extends infinitely along x and y directions, and has a thickness h. The polarization direction of the transversely isotropic piezoelectric plate is along z-axis perpendicular to the x–y plate. The wave propagates along the positive direction of x-axis with phase velocity c. The biasing voltage is applied to the upper surface of the plate while the lower surface is grounded. The biasing field is applied parallel to the thickness direction. When the biasing electric field is applied, the components of initial stress and initial electric displacement exist in the plate, and hence the phase velocity of Lamb waves is changed through electroacoustic effects. Initial stresses and initial electric displacements should satisfy the constitutive equations in the initial reference configuration, i.e.,

$$\sigma_x^0 = c_{11}S_x^0 + c_{12}S_y^0 + c_{13}S_z^0 - e_{31}E_z^0 \tag{1a}$$

$$\sigma_y^0 = c_{12}S_x^0 + c_{11}S_y^0 + c_{13}S_z^0 - e_{31}E_z^0 \tag{1b}$$

$$\sigma_z^0 = c_{13}S_x^0 + c_{13}S_y^0 + c_{33}S_z^0 - e_{33}E_z^0 \tag{1c}$$

$$D_x^0 = e_{15}S_{zx}^0 + \varepsilon_{11}E_x^0 \tag{1d}$$

$$D_y^0 = e_{15}S_{yz}^0 + \varepsilon_{11}E_z^0 \tag{1e}$$

$$D_z^0 = e_{31}S_x^0 + e_{31}S_y^0 + e_{33}S_z^0 + \varepsilon_{33}E_z^0 \tag{1f}$$

where σ_x^0, σ_y^0 and σ_z^0 are initial stresses, D_x^0, D_y^0 and D_z^0 are initial electric displacements, S_x^0, S_y^0, S_z^0, S_{zx}^0 and S_{yz}^0 are initial strains, E_x^0, E_y^0, E_z^0 are initial electric fields, c_{11}, c_{12}, c_{13} and c_{33} are elastic constants, e_{31}, e_{33} and e_{15} are piezoelectric constants, ε_{11} and ε_{33} are dielectric constants of the transversely isotropic piezoelectric plate.

We assume that there exists only one constant initial stress component σ_x^0 in the plate, and the other components of the initial stress are zero. For the plain strain problem, $S_y^0 = 0$. Considering the thin plate, we have $\sigma_z^0 = 0$. From the third equation of Eqs. (1a)–(1f) we have

$$S_z^0 = -\frac{c_{13}}{c_{33}}S_x^0 + \frac{e_{33}}{c_{33}}E_z^0$$

then substitute this equation into Eqs. (1a) and (1f), we obtain

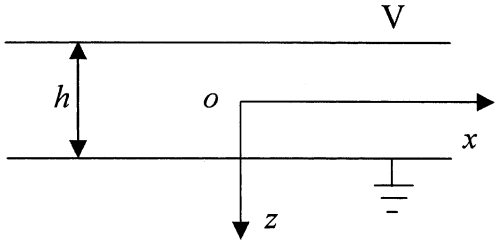

Fig. 1. Infinite piezoelectric plate in a biasing electric field.

$$\sigma_x^0 = \left(c_{11} - \frac{c_{13}^2}{c_{33}}\right) S_x^0 + \left(\frac{c_{13}e_{33}}{c_{33}} - e_{31}\right) E_z^0 \tag{2a}$$

$$D_z^0 = \left(e_{31} - \frac{c_{13}e_{33}}{c_{33}}\right) S_x^0 + \left(\frac{e_{33}^2}{c_{33}} + \varepsilon_{33}\right) E_z^0 \tag{2b}$$

Because the media is an insulator and no free charge exists, the electric displacements satisfy the Gaussian equation, and the electric field E_z^0 is related to the initial electrical potential φ^0, i.e.,

$$\frac{\partial D_x^0}{\partial x} + \frac{\partial D_y^0}{\partial y} + \frac{\partial D_z^0}{\partial z} = 0 \tag{3a}$$

$$E_z^0 = -\frac{\partial \varphi^0}{\partial z} \tag{3b}$$

When the biasing voltage V is applied only along the z direction, we have $S_x^0 = 0$, $D_x^0 = D_y^0 = 0$. Considering these conditions, we can obtain from Eqs. (3a) and (3b) that yields

$$\frac{\partial^2 \varphi^0}{\partial z^2} = 0 \tag{4}$$

The solution of Eq. (4) is $\varphi^0 = az + q$, where a and q are unknown constants. From the electrical boundary conditions, it can be stated that

$$a \cdot \left(-\frac{h}{2}\right) + q = V \tag{5a}$$

and

$$a \cdot \left(\frac{h}{2}\right) + q = 0 \tag{5b}$$

We have

$$\varphi^0 = -\frac{V}{h} \cdot z + \frac{V}{2} \tag{6}$$

Substitution of (6) into Eq. (3b), yields

$$E_z^0 = -\frac{\partial \varphi^0}{\partial z} = \frac{V}{h} \tag{7}$$

Substitution of Eq. (7) into Eqs. (2a) and (2b) yields the initial stress and initial displacement produced by the biasing voltage

$$\sigma_x^0 = \left(\frac{c_{13}e_{33}}{c_{33}} - e_{31}\right) \cdot \frac{V}{h} \tag{8a}$$

$$D_z^0 = \left(\frac{e_{33}^2}{c_{33}} + \varepsilon_{33}\right) \cdot \frac{V}{h} \tag{8b}$$

2.2. Governing equations

The field equations of the piezoelectric body with initial stresses can be expressed as (Wang and Shang, 1997)

$$\sigma_{ij,j} + (u_{i,k} \cdot \sigma^0_{kj})_{,j} = \rho \cdot \ddot{u}_i \tag{9a}$$

$$D_{i,i} + (u_{i,j} \cdot D^0_j)_{,i} = 0 \tag{9b}$$

where i, j, $k = 1, 2, 3$, ρ is mass density, u_i and D_i denote the mechanical displacement and the electric displacement in the ith direction, respectively, σ_{ij} is stress tensor. For the plain strain problem, displacements u, v, w and electrical potential φ should satisfy

$$u = u(x, z, t) \tag{10a}$$

$$v = 0 \tag{10b}$$

$$w = w(x, z, t) \tag{10c}$$

$$\varphi = \varphi(x, z, t) \tag{10d}$$

Substitution of Eqs. (10a)–(10d) into Eqs. (9a) and (9b), we have

$$\frac{\partial \sigma_x}{\partial x} + \frac{\partial \tau_{zx}}{\partial z} + \sigma^0_x \frac{\partial^2 u}{\partial x^2} = \rho \frac{\partial^2 u}{\partial t^2} \tag{11a}$$

$$\frac{\partial \tau_{zx}}{\partial x} + \frac{\partial \sigma_z}{\partial z} + \sigma^0_x \frac{\partial^2 w}{\partial x^2} = \rho \frac{\partial^2 w}{\partial t^2} \tag{11b}$$

$$\frac{\partial D_x}{\partial x} + \frac{\partial D_z}{\partial z} + D^0_z \frac{\partial^2 u}{\partial x \partial z} + D^0_z \frac{\partial^2 w}{\partial z^2} = 0 \tag{11c}$$

From the constitutive equations of the transversely isotropic piezoelectric media,

$$\sigma_x = c_{11} S_x + c_{13} S_z - e_{31} E_z \tag{12a}$$

$$\sigma_y = c_{12} S_x + c_{13} S_z - e_{33} E_z \tag{12b}$$

$$\sigma_z = c_{13} S_x + c_{33} S_z - e_{33} E_z \tag{12c}$$

$$\tau_{zx} = c_{44} S_{zx} - e_{15} E_x \tag{12d}$$

$$D_x = e_{15} S_{zx} + \varepsilon_{11} E_x \tag{12e}$$

$$D_z = e_{31} S_x + e_{33} S_z + \varepsilon_{33} E_z \tag{12f}$$

where

$$S_x = \frac{\partial u}{\partial x}, \quad S_y = \frac{\partial v}{\partial y}, \quad S_z = \frac{\partial w}{\partial z}, \quad S_{yz} = \frac{\partial w}{\partial y} + \frac{\partial v}{\partial z}, \quad S_{zx} = \frac{\partial u}{\partial z} + \frac{\partial w}{\partial x}$$

$$S_{xy} = \frac{\partial u}{\partial y} + \frac{\partial v}{\partial x}, \quad E_x = -\frac{\partial \varphi}{\partial x}, \quad E_y = -\frac{\partial \varphi}{\partial y}, \quad E_z = -\frac{\partial \varphi}{\partial z}$$

Substitution of Eqs. (12a)–(12f) and Eqs. (8a) and (8b) into Eqs. (11a)–(11c), we have

$$\left[c_{11} + \left(\frac{c_{13} e_{33}}{c_{33}} - e_{31}\right) \frac{V}{h}\right] \cdot \frac{\partial^2 u}{\partial x^2} + c_{44} \frac{\partial^2 u}{\partial z^2} + (c_{13} + c_{44}) \frac{\partial^2 w}{\partial x \partial z} + (e_{31} + e_{15}) \frac{\partial^2 \varphi}{\partial x \partial z} = \rho \frac{\partial^2 u}{\partial t^2} \tag{13a}$$

$$(c_{13} + c_{44}) \frac{\partial^2 u}{\partial x \partial z} + \left[c_{44} + \left(\frac{c_{13} e_{33}}{c_{33}} - e_{31}\right) \frac{V}{h}\right] \cdot \frac{\partial^2 w}{\partial x^2} + c_{33} \frac{\partial^2 w}{\partial z^2} + e_{15} \frac{\partial^2 \varphi}{\partial x^2} + e_{33} \frac{\partial^2 \varphi}{\partial z^2} = \rho \frac{\partial^2 w}{\partial t^2} \tag{13b}$$

$$\left[e_{15}+e_{31}+\left(\frac{e_{33}^2}{c_{33}}+\varepsilon_{33}\right)\frac{V}{h}\right]\frac{\partial^2 u}{\partial x\partial z}+e_{15}\frac{\partial^2 w}{\partial x^2}+\left[e_{33}+\left(\frac{e_{33}^2}{c_{33}}+\varepsilon_{33}\right)\frac{V}{h}\right]\frac{\partial^2 w}{\partial z^2}-\varepsilon_{11}\frac{\partial^2\varphi}{\partial x^2}-\varepsilon_{33}\frac{\partial^2\varphi}{\partial z^2}=0 \tag{13c}$$

Usually, the piezoelectric layer is in air. The dielectric constant (ε_0) of air is very small compared to that of the piezoelectric medium. Thus, the air can be treated as vacuum, such that the electric potential φ_0 for the air satisfies Laplace's equation,

$$\frac{\partial^2\varphi_0}{\partial x^2}+\frac{\partial^2\varphi_0}{\partial z^2}=0 \tag{14}$$

When Lamb waves propagate in the plate, as shown in Fig. 1, both the components of mechanical displacement and the electrical potential must satisfy Eqs. (13a)–(13c) and (14). Moreover, the related mechanical and electrical variables must satisfy the boundary conditions, which are described as follows.

(I) The mechanical traction-free conditions at $z=\pm h/2$

$$\tau_{zx}\left(x,\pm\frac{h}{2}\right)=0$$

$$\sigma_z\left(x,\pm\frac{h}{2}\right)=0$$

(II) The electrical boundary conditions for electrically open case at $z=\pm h/2$

$$\varphi_0\left(x,\pm\frac{h}{2}\right)=\varphi\left(x,\pm\frac{h}{2}\right)$$

$$D_{z0}\left(x,\pm\frac{h}{2}\right)=D_z\left(x,\pm\frac{h}{2}\right)$$

(III) The electrical boundary conditions for electrically shorted case at $z=\pm h/2$

$$\varphi\left(x,\pm\frac{h}{2}\right)=0$$

3. Symmetric modes (OPS)

3.1. Solutions of the mechanical displacements and electrical potential

For the OPS mode, we assume the solutions of Eqs. (13a)–(13c) as (Romos and Otero, 1997)

$$u=B_1\cos(kbz)\exp[\mathrm{i}k(x-ct)] \tag{15a}$$

$$w=B_2\sin(kbz)\exp[\mathrm{i}k(x-ct)] \tag{15b}$$

$$\varphi=B_3\sin(kbz)\exp[\mathrm{i}k(x-ct)] \tag{15c}$$

where B_1, B_2 and B_3 are constants determined by the excitation, k is wave number and $k=2\pi/\lambda$, λ is wavelength, b is constant, $\mathrm{i}=\sqrt{-1}$.

Substitution of Eqs. (15a)–(15c) into Eqs. (13a)–(13c), yields

$$-\left[c_{11}-\rho c^2+c_{44}b^2+\left(\frac{c_{13}e_{33}}{c_{33}}-e_{31}\right)\frac{V}{h}\right]B_1+(c_{13}+c_{44})b\mathrm{i}B_2+(e_{31}+e_{15})b\mathrm{i}B_3=0 \tag{16a}$$

$$(c_{13}+c_{44})b\mathrm{i}B_1+\left[c_{44}-\rho c^2+c_{33}b^2+\left(\frac{c_{13}e_{33}}{c_{33}}-e_{31}\right)\frac{V}{h}\right]B_2+(e_{15}+e_{33}b^2)B_3=0 \tag{16b}$$

$$\left[e_{15}+e_{31}+\left(\frac{e_{33}^2}{c_{33}}+\varepsilon_{33}\right)\frac{V}{h}\right]b\mathrm{i}B_1+\left\{e_{15}+\left[e_{33}+\left(\frac{e_{33}^2}{c_{33}}+\varepsilon_{33}\right)\frac{V}{h}\right]b^2\right\}B_2-(\varepsilon_{11}+\varepsilon_{33}b^2)B_3=0 \tag{16c}$$

In order to get nontrivial solution, the determinant of the coefficient matrix of Eqs. (16a)–(16c) must be equal to zero, i.e.

$$\begin{vmatrix} -\left[c_{11}-\rho c^2+c_{44}b^2+\left(\frac{c_{13}e_{33}}{c_{33}}-e_{31}\right)\frac{V}{h}\right] & (c_{13}+c_{44})b\mathrm{i} & (e_{31}+e_{15})b\mathrm{i} \\ (c_{13}+c_{44})b\mathrm{i} & c_{44}-\rho c^2+c_{33}b^2+\left(\frac{c_{13}e_{33}}{c_{33}}-e_{31}\right)\frac{V}{h} & (e_{15}+e_{33}b^2) \\ \left[e_{15}+e_{31}+\left(\frac{e_{33}^2}{c_{33}}+\varepsilon_{33}\right)\frac{V}{h}\right]b\mathrm{i} & e_{15}+\left[e_{33}+\left(\frac{e_{33}^2}{c_{33}}+\varepsilon_{33}\right)\frac{V}{h}\right]b^2 & -(\varepsilon_{11}+\varepsilon_{33}b^2) \end{vmatrix}=0 \tag{17}$$

Eq. (17) is a third-order equation in b^2 with phase velocity c as the unknown parameter. For every value of c, biasing voltage V and material constants, there are three solutions b_n^2 ($n=1$–3). The roots $+b_n$ and $-b_n$ do not yield independent solutions on account of the form of Eqs. (15a)–(15c). So only three solutions of b_n ($n=1$–3) are adopted. The cubic equation for (17) is:

$$A_3(b^2)^3+A_2(b^2)^2+A_1(b^2)+A_0=0$$

where

$$A_3=c_{44}\left[c_{33}\varepsilon_{33}+e_{33}^2+e_{33}\left(\frac{e_{33}^2}{c_{33}}+\varepsilon_{33}\right)\frac{V}{h}\right]$$

$$\begin{aligned}A_2=&-2e_{33}(c_{13}+c_{44})(e_{31}+e_{15})-\left(\frac{e_{33}^2}{c_{33}}+\varepsilon_{33}\right)\frac{V}{h}(c_{13}+c_{44})(e_{33}+e_{31}+e_{15})\\&+c_{44}\left\{\varepsilon_{33}\left[c_{44}-\rho c^2+\left(\frac{c_{13}e_{33}}{c_{33}}-e_{31}\right)\frac{V}{h}\right]+2e_{15}e_{33}+\varepsilon_{11}c_{33}+\left(\frac{e_{33}^2}{c_{33}}+\varepsilon_{33}\right)\frac{V}{h}e_{15}\right\}\\&+c_{33}(e_{31}+e_{15})\left[e_{31}+e_{15}+\left(\frac{e_{33}^2}{c_{33}}+\varepsilon_{33}\right)\frac{V}{h}\right]-\varepsilon_{33}(c_{13}+c_{44})^2+\left[c_{33}\varepsilon_{33}+e_{33}^2+e_{33}\left(\frac{e_{33}^2}{c_{33}}+\varepsilon_{33}\right)\frac{V}{h}\right]\\&\times\left[c_{11}-\rho c^2+\left(\frac{c_{13}e_{33}}{c_{33}}-e_{31}\right)\frac{V}{h}\right]\end{aligned}$$

$$\begin{aligned}A_1=&\left[c_{11}-\rho c^2+\left(\frac{c_{13}e_{33}}{c_{33}}-e_{31}\right)\frac{V}{h}\right]\cdot\left\{\varepsilon_{33}\cdot\left[c_{44}-\rho c^2+\left(\frac{c_{13}e_{33}}{c_{33}}-e_{31}\right)\frac{V}{h}\right]\right.\\&\left.+\varepsilon_{11}c_{33}+2e_{15}e_{33}-e_{15}\cdot\left(\frac{e_{33}^2}{c_{33}}+\varepsilon_{33}\right)\frac{V}{h}\right\}+c_{44}e_{15}^2+\left\{c_{44}\varepsilon_{11}+(e_{15}+e_{31})\cdot\left[(e_{15}+e_{31})\right.\right.\\&\left.\left.+\left(\frac{e_{33}^2}{c_{33}}+\varepsilon_{33}\right)\frac{V}{h}\right]\right\}\cdot\left[c_{44}-\rho c^2+\left(\frac{c_{13}e_{33}}{c_{33}}-e_{31}\right)\frac{V}{h}\right]-\varepsilon_{11}(c_{13}+c_{44})^2\\&-2e_{15}(c_{13}+c_{44})(e_{15}+e_{31})+e_{15}(c_{13}+c_{44})\left(\frac{e_{33}^2}{c_{33}}+\varepsilon_{33}\right)\frac{V}{h}\end{aligned}$$

$$A_0 = \left[c_{11} - \rho c^2 + \left(\frac{c_{13}e_{33}}{c_{33}} - e_{31}\right)\frac{V}{h}\right] \cdot \left\{e_{15}^2 + \varepsilon_{11} \cdot \left[c_{44} - \rho c^2 + \left(\frac{c_{13}e_{33}}{c_{33}} - e_{31}\right)\frac{V}{h}\right]\right\}$$

when substituted in any two of Eq. (17), each independent b_n ($n = 1$–3) yields the amplitude ratios B_{1n}/B_{3n}, B_{2n}/B_{3n} ($n = 1$–3), i.e.,

$$\frac{B_{1n}}{B_{3n}} = \frac{-(e_{31}+e_{15}) \cdot \left[c_{44} - \rho c^2 + c_{33}b_n^2 + \left(\frac{c_{13}e_{33}}{c_{33}} - e_{31}\right)\frac{V}{h}\right] + (e_{15} + e_{33}b_n^2)(c_{13}+c_{44})}{-\left[c_{11} - \rho c^2 + c_{44}b_n^2 + \left(\frac{c_{13}e_{33}}{c_{33}} - e_{31}\right)\frac{V}{h}\right] \cdot \left[c_{44} - \rho c^2 + c_{33}b_n^2 + \left(\frac{c_{13}e_{33}}{c_{33}} - e_{31}\right)\frac{V}{h}\right] + (c_{13}+c_{44})^2 b_n^2} \times b_n \cdot \mathrm{i} = F_{1n} \tag{18a}$$

$$\frac{B_{2n}}{B_{3n}} = \frac{\left[c_{11} - \rho c^2 + c_{44}b_n^2 - \left(\frac{c_{13}e_{33}}{c_{33}} + e_{31}\right)\frac{V}{h}\right] \cdot (e_{15} + e_{33}b_n^2) - (c_{13}+c_{44})(e_{31}+e_{15})b_n^2}{-\left[c_{11} - \rho c^2 + c_{44}b_n^2 + \left(\frac{c_{13}e_{33}}{c_{33}} - e_{31}\right)\frac{V}{h}\right] \cdot \left[c_{44} - \rho c^2 + c_{33}b_n^2 + \left(\frac{c_{13}e_{33}}{c_{33}} - e_{31}\right)\frac{V}{h}\right] + (c_{13}+c_{44})^2 b_n^2} = F_{2n} \tag{18b}$$

Substitution of Eqs. (18a) and (18b) into Eqs. (15a)–(15c), the displacement and electrical potential for OPS are rewritten as

$$u = \sum_{n=1}^{3} F_{1n}B_{3n}\cos(kb_n z)\exp[\mathrm{i}k(x-ct)] \tag{19a}$$

$$w = \sum_{n=1}^{3} F_{2n}B_{3n}\sin(kb_n z)\exp[\mathrm{i}k(x-ct)] \tag{19b}$$

$$\varphi = \sum_{n=1}^{3} B_{3n}\sin(kb_n z)\exp[\mathrm{i}k(x-ct)] \tag{19c}$$

In addition, the solutions of electrical potential in the vacuum can be obtained from Eq. (14), i.e.,

$$\varphi_0 = B_4 \mathrm{e}^{-kz} \cdot \exp[\mathrm{i}k(x-ct)] \quad (z \geqslant h/2) \tag{20}$$

3.2. Solutions of the phase velocity

3.2.1. Electrically open case

Substituting Eqs. (19a)–(19c) and (20) and their corresponding components of stress and electrical displacement into the boundary conditions (I) and (II), we can obtain the algebraic equations in the unknown constants B_{31}, B_{32}, B_{33}, and B_4. After simplifying, we can obtain the algebraic equations in the unknown constants B_{31}, B_{32}, and B_{33}, i.e.,

$$[P][B] = 0 \tag{21}$$

where $[P]$ is a 3×3 matrix, P_{sn} ($s = 1$–$3, n = 1$–3) are given by

$$P_{1n} = [c_{44}(F_{2n} \cdot \mathrm{i} - b_n F_{1n}) + e_{15} \cdot \mathrm{i}] \cdot \sin\left(kb_n \frac{h}{2}\right)$$

$$P_{2n} = (c_{13}F_{1n} \cdot \mathrm{i} + c_{33}b_n F_{2n} + e_{33}b_n) \cdot \cos\left(kb_n \frac{h}{2}\right)$$

$$P_{3n} = \frac{1}{\varepsilon_0}(e_{31}F_{1n}\cdot \mathrm{i} + e_{33}b_nF_{2n} - \varepsilon_{33}b_n)\cos\left(kb_n\frac{h}{2}\right) - \sin\left(kb_n\frac{h}{2}\right)$$

Let

$$d_1 = c_{44}(F_{21}\cdot \mathrm{i} - b_1F_{11}) + e_{15}\cdot \mathrm{i}, \quad d_2 = c_{44}(F_{22}\cdot \mathrm{i} - b_2F_{12}) + e_{15}\cdot \mathrm{i}$$

$$d_3 = c_{44}(F_{23}\cdot \mathrm{i} - b_3F_{13}) + e_{15}\cdot \mathrm{i}, \quad f_1 = c_{13}F_{11}\cdot \mathrm{i} + c_{33}b_1F_{21} + e_{33}b_1$$

$$f_2 = c_{13}F_{12}\cdot \mathrm{i} + c_{33}b_2F_{22} + e_{33}b_2, \quad f_3 = c_{13}F_{13}\cdot \mathrm{i} + c_{33}b_3F_{23} + e_{33}b_3$$

$$g_1 = \frac{1}{\varepsilon_0}(e_{31}F_{11}\cdot \mathrm{i} + e_{33}b_1F_{21} - \varepsilon_{33}b_1), \quad g_2 = \frac{1}{\varepsilon_0}(e_{31}F_{12}\cdot \mathrm{i} + e_{33}b_2F_{22} - \varepsilon_{33}b_2)$$

$$g_3 = \frac{1}{\varepsilon_0}(e_{31}F_{13}\cdot \mathrm{i} + e_{33}b_3F_{23} - \varepsilon_{33}b_3)$$

To obtain a nontrivial solution, the determinant of the coefficient matrix must be equal to zero, i.e.,

$$\mathrm{tg}(\pi m b_1)\cdot[e_1\mathrm{tg}(\pi m b_2) - h_2] + \mathrm{tg}(\pi m b_2)\cdot[e_3\mathrm{tg}(\pi m b_3) - h_2] + \mathrm{tg}(\pi m b_3)\cdot[e_2\mathrm{tg}(\pi m b_1) - h_3] = 0 \tag{22}$$

where

$$m = h/\lambda, \quad e_1 = f_3(d_2 - d_1), \quad e_2 = f_2(d_1 - d_3), \quad e_3 = f_1(d_3 - d_2), \quad h_1 = d_1(f_2g_3 - f_3g_2),$$
$$h_2 = d_2(f_3g_1 - f_1g_3), \quad h_3 = d_3(f_1g_2 - f_2g_1)$$

m is a ratio of plate thickness to wavelength. Generally, Lamb waves are excited by an interdigital transducer (IDT) deposited on the piezoelectric plate. The wavelength λ equals to the spatial periodicity of the IDTs. Also, the thickness of the plate can be accurately measured. Thus the value of m can be defined. It is a very important variable in SAW devices, the wave modes that a plate supports depend on the value of the ratio h/λ.

In addition, for the electrically open case, the biasing voltage V in Eqs. (16a)–(16c) and (17) should be equal to zero.

3.2.2. Electrically shorted case

Substituting Eqs. (20) and (19a)–(19c) and relevant components of stress and electrical displacement into boundary conditions (I) and (III), we obtain the algebraic equations in the unknown constants B_{31}, B_{32} and B_{33}, i.e.,

$$[P][B] = 0 \tag{23}$$

where $[P]$ is a 3×3 matrix, P_{sn} $(s = 1\text{–}3, n = 1\text{–}3)$ are given by

$$P_{1n} = [c_{44}(F_{2n}\cdot \mathrm{i} - b_nF_{1n}) + e_{15}\cdot \mathrm{i}]\cdot\sin\left(kb_n\frac{h}{2}\right)$$

$$P_{2n} = (c_{13}F_{1n}\cdot \mathrm{i} + c_{33}b_nF_{2n} + e_{33}b_n)\cdot\cos\left(kb_n\frac{h}{2}\right)$$

$$P_{3n} = \sin\left(kb_n\frac{h}{2}\right)$$

Then we can get a similar solution of phase velocity for the electrically shorted case

$$e_1\mathrm{tg}(\pi m b_1)\,\mathrm{tg}(\pi m b_2) + e_2\mathrm{tg}(\pi m b_1)\,\mathrm{tg}(\pi m b_3) + e_3\mathrm{tg}(\pi m b_2)\,\mathrm{tg}(\pi m b_3) = 0 \tag{24}$$

Due to the complexity of problem, numerical search routine is necessary to find the root of phase velocity that lets $|P|$ vanish.

3.3. Solutions of the stress field

After the root of the phase velocity is found, for both electrically open and shorted cases, from the first two equations of boundary equations, we have

$$B_{31} = \beta_1 B_{33}, \quad B_{32} = \beta_2 B_{33}, \quad B_{33} = \beta_3 B_{33} \tag{25}$$

where

$$\beta_1 = \frac{-\sin(\pi m b_3) d_3 \cdot \cos(\pi m b_2) f_2 + \sin(\pi m b_2) d_2 \cos(\pi m b_3) f_3}{\sin(\pi m b_1) d_1 \cdot \cos(\pi m b_2) f_2 - \sin(\pi m b_2) d_2 \cos(\pi m b_1) f_1}$$

$$\beta_2 = \frac{-\sin(\pi m b_1) d_1 \cdot \cos(\pi m b_3) f_3 + \sin(\pi m b_3) d_3 \cdot \cos(\pi m b_1) f_1}{\sin(\pi m b_1) d_1 \cdot \cos(\pi m b_2) f_2 - \sin(\pi m b_2) d_2 \cdot \cos(\pi m b_1) f_1}$$

$$\beta_3 = 1$$

The value of B_{33} is determined by the excitation. Substitution of Eq. (25) into Eqs. (19a)–(19c), yields

$$u = \left[\sum_{n=1}^{3} F_{1n} \beta_n \cos(k b_n z) \right] \cdot B_{33} \cdot \exp[\mathrm{i} k (x - ct)] \tag{26a}$$

$$w = \left[\sum_{n=1}^{3} F_{2n} \beta_n \sin(k b_n z) \right] \cdot B_{33} \cdot \exp[\mathrm{i} k (x - ct)] \tag{26b}$$

$$\varphi = \left[\sum_{n=1}^{3} \beta_n \sin(k b_n z) \right] \cdot B_{33} \cdot \exp[\mathrm{i} k (x - ct)] \tag{26c}$$

Substituting Eqs. (26a)–(26c) into Eqs. (12a)–(12f), solutions of the stress fields are expressed as

$$\tau_{zx} = \left\{ \sum_{n=1}^{3} [c_{44}(F_{2n} \cdot \mathrm{i} - b_n F_{1n}) + e_{15} \cdot \mathrm{i}] \cdot k \cdot \beta_n \cdot \sin(k b_n z) \right\} \cdot B_{33} \cdot \exp[\mathrm{i} k (x - ct)] \tag{27a}$$

$$\sigma_z = \left[\sum_{n=1}^{3} (c_{13} F_{1n} \cdot \mathrm{i} + c_{33} b_n F_{2n} + e_{33} b_n) \cdot k \cdot \beta_n \cdot \cos(k b_n z) \right] \cdot B_{33} \cdot \exp[\mathrm{i} k (x - ct)] \tag{27b}$$

$$\sigma_x = \left[\sum_{n=1}^{3} (c_{11} F_{1n} \cdot \mathrm{i} + c_{13} b_n F_{2n} + e_{31} b_n) \cdot k \cdot \beta_n \cdot \cos(k b_n z) \right] \cdot B_{33} \cdot \exp[\mathrm{i} k (x - ct)] \tag{27c}$$

$$\sigma_y = \left[\sum_{n=1}^{3} (c_{12} F_{1n} \cdot \mathrm{i} + c_{13} b_n F_{2n} + e_{31} b_n) \cdot k \cdot \beta_n \cdot \cos(k b_n z) \right] \cdot B_{33} \cdot \exp[\mathrm{i} k (x - ct)] \tag{27d}$$

4. Discussions

To graphically show the effect of a biasing electric field on the phase velocity, electromechanical coupling coefficient, displacements and stress fields of the first several symmetric Lamb wave modes, calculations are performed for several materials. The results show essentially similar behavior, so only the calculated results of PZT-5H ceramics are given. The material constants of PZT-5H ceramics are taken from Ristic (1983), as shown in Table 1. The dielectric constant of vacuum is $\varepsilon_0 = 8.85 \times 10^{-12}$ F/m. The plate thickness is 0.5 mm.

For displaying the amplitudes of mechanical displacements and stress components as a function of z, it is necessary for us to take the real part of their expressions (Mesquida et al., 1998). Let χ denote all these variables, then

$$\chi(x,z,t) = \overline{\chi}(z)\exp[\mathrm{i}k(x-ct)]$$

This leads to

$$\mathrm{Re}[\chi(x,z,t)] = \sqrt{\{\mathrm{Re}[\overline{\chi}(z)]\}^2 + \{\mathrm{Im}[\overline{\chi}(z)]\}^2} \times \cos[k(x-ct)+\alpha]$$

where

$$\alpha = \mathrm{arctg}\left(\frac{\mathrm{Im}[\bar{\chi}(z)]}{\mathrm{Re}[\bar{\chi}(z)]}\right)$$

Generally, we plot $\mathrm{Im}[\bar{\chi}(z)]$ and $\mathrm{Re}[\bar{\chi}(z)]$ to show the z dependence of the amplitude of χ.

4.1. Effect of the biasing electric field on the phase velocity and electromechanical coupling coefficient

The phase velocity c of the first several symmetric modes can be calculated from equations in Section 3 for electrically open and shorted cases, respectively, with different values of m and biasing electric field. Here m is the ratio of plate thickness to wavelength, a very important parameter for SAW, changes from 0.01 to 3. The breakdown fields of ceramics are of the order of 4–60 kV/mm (Xu, 1993). Here we assume the plate is under a biasing electric field of 2.5 kV/mm without breakdown. Effects of the biasing electric field on the fractional change in phase velocity $\Delta c/c$ are shown in Fig. 2. Fig. 2(a)–(c) are shown for the s_0 mode, s_1 mode and s_2 mode of Lamb wave in turn. In Fig. 2, the horizontal axis is the biasing electric field, the vertical axis is the fractional change in phase velocity. It is shown that the biasing electric field has significant effects on the phase velocity of symmetric Lamb waves. The phase velocity increases when the biasing electric field changes from -2.5 to 2.5 kV/mm. The maximum fractional velocity change $\Delta c/c$ that we obtained is 0.1% corresponding to a biasing electric field of 2.5 kV/mm at $m = 3.00$ for the s_0 mode. The

Table 1
Material constants

Material	Elastic constant (10^{10} N/m^2)					Mass density ρ (kg/m^3)	Piezoelectric constant (C/m^2)			Dielectric constant (10^{-10} F/m)	
	c_{11}	c_{12}	c_{13}	c_{33}	c_{44}		e_{15}	e_{31}	e_{33}	ε_{11}	ε_{33}
PZT-5H ceramics	12.1	7.95	8.41	11.7	2.30	7.5	17.0	−6.5	23.3	150	130
PZT-2 ceramics	13.5	6.79	6.81	11.3	2.22	7.6	9.8	−1.9	9.0	44.6	23.0
Lead-oxide glass	6.13				2.18	3.879				0.36	0.36
SiO_2 glass	7.85				3.12	2.2				0.33	0.33
Borosilicate glass	7.42				2.78	2.23				0.45	0.45
ZnO	20.96	12.11	10.51	21.09	4.25	5.68	−0.48	−0.573	1.32	0.75	0.90

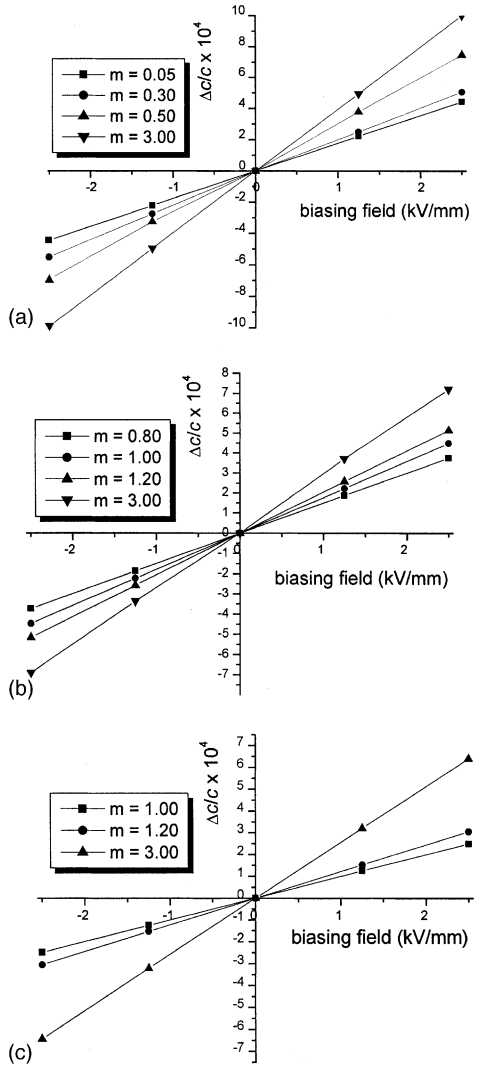

Fig. 2. Variations of the fractional phase velocity change vs. the biasing electric field for Lamb waves in a PZT-5H ceramic plate, (a) s_0 mode, (b) s_1 mode and (c) s_2 mode.

fractional velocity changes enhance with the increase of the ratio of the plate thickness to wavelength. This result is very useful for designing acoustic devices, for example, the delay time of delay lines is related to the phase velocity, which can be altered by applying proper biasing electric fields according to Fig. 2. Thus, in order to obtain a large variation of time delay, one can apply a biasing electric field.

The dispersion relations for the s_0, s_1 and s_2 modes for electrically open case are plotted in Fig. 3. It is seen that as $k \to \infty$, the velocity of the s_0 mode tends to the free-surface Rayleigh velocity. The velocity of the higher modes is asymptotic to the bulk shear velocity.

From Figs. 2 and 3, we can calculate the electromechanical coupling coefficient K^2 for the determination of the most efficient structure. As we known, the original definition of K^2 is related with energy, and expressed as (Laurent et al., 2000)

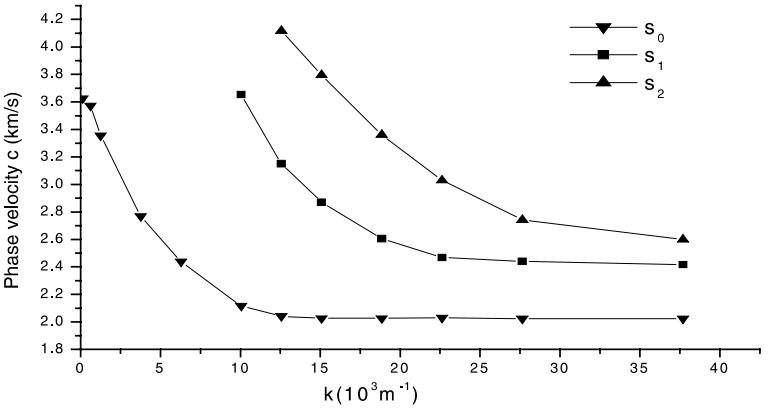

Fig. 3. For the electrically open case, the dispersion relations for the s_0, s_1 and s_2 modes of PZT-5H ceramics.

$$K^2 = U_m^2/(U_c U_d)$$

where U_m is the mutual electric and mechanical energy, U_c is the dielectric energy and U_d the mechanical energy. For general SAW devices, the electromechanical coupling coefficient K^2, which is a very important parameter of piezoelectric devices, is defined as

$$K^2 = 2\frac{c_f - c_0}{c_f}$$

where c_f and c_0 are the phase velocities for electrically open and shorted cases, respectively. However, Lamb waves are not surface acoustic waves. Only for larger ratios of plate thickness to wavelength, and when the velocities of in-phase a_0 and s_0 modes tend to the Rayleigh wave velocity, the sum of a_0 and s_0 Lamb modes with equal amplitudes can be thought as Rayleigh modes on the surface mode, the difference of a_0 and s_0 Lamb modes can be thought as Rayleigh modes on the bottom surface of the plate. So the above equation can not be applied to calculate the electromechanical coupling coefficient, we can define it as a factor to reflect the change of velocity after metalizing and therefore we obtain a rough result. From Fig. 4, it is seen that for $m = 3.0$, K^2 can be increased by the negative biasing electric field. It can be

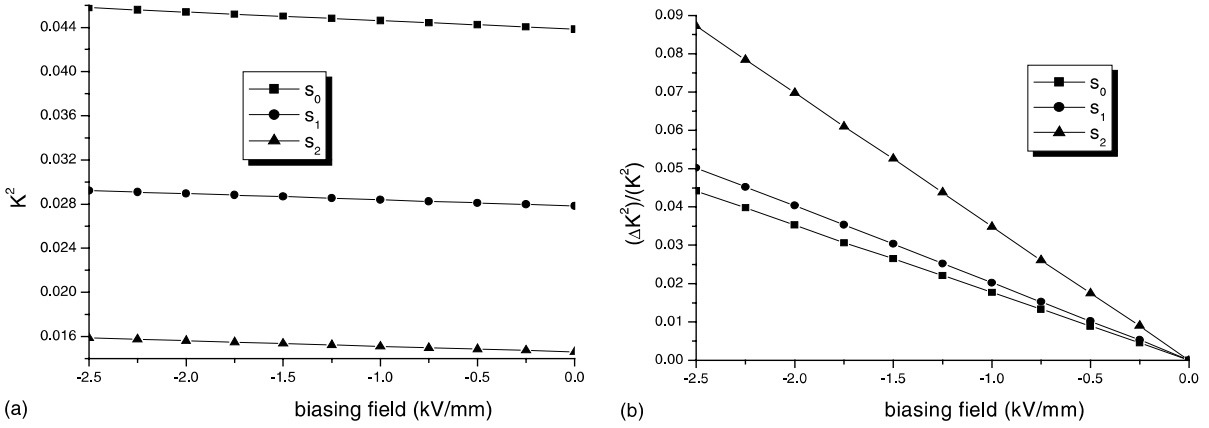

Fig. 4. The electromechanical coupling factor at $m = 3.0$, (a) K^2 and (b) $(\Delta K^2)/(K^2)$.

observed from Fig. 4(a) that the electromechanical coupling coefficient for the s_0 mode attains highest values. The maximum is 0.04579 under a biasing electric field of -2.5 kV/mm. Fig. 4(b) illustrates the

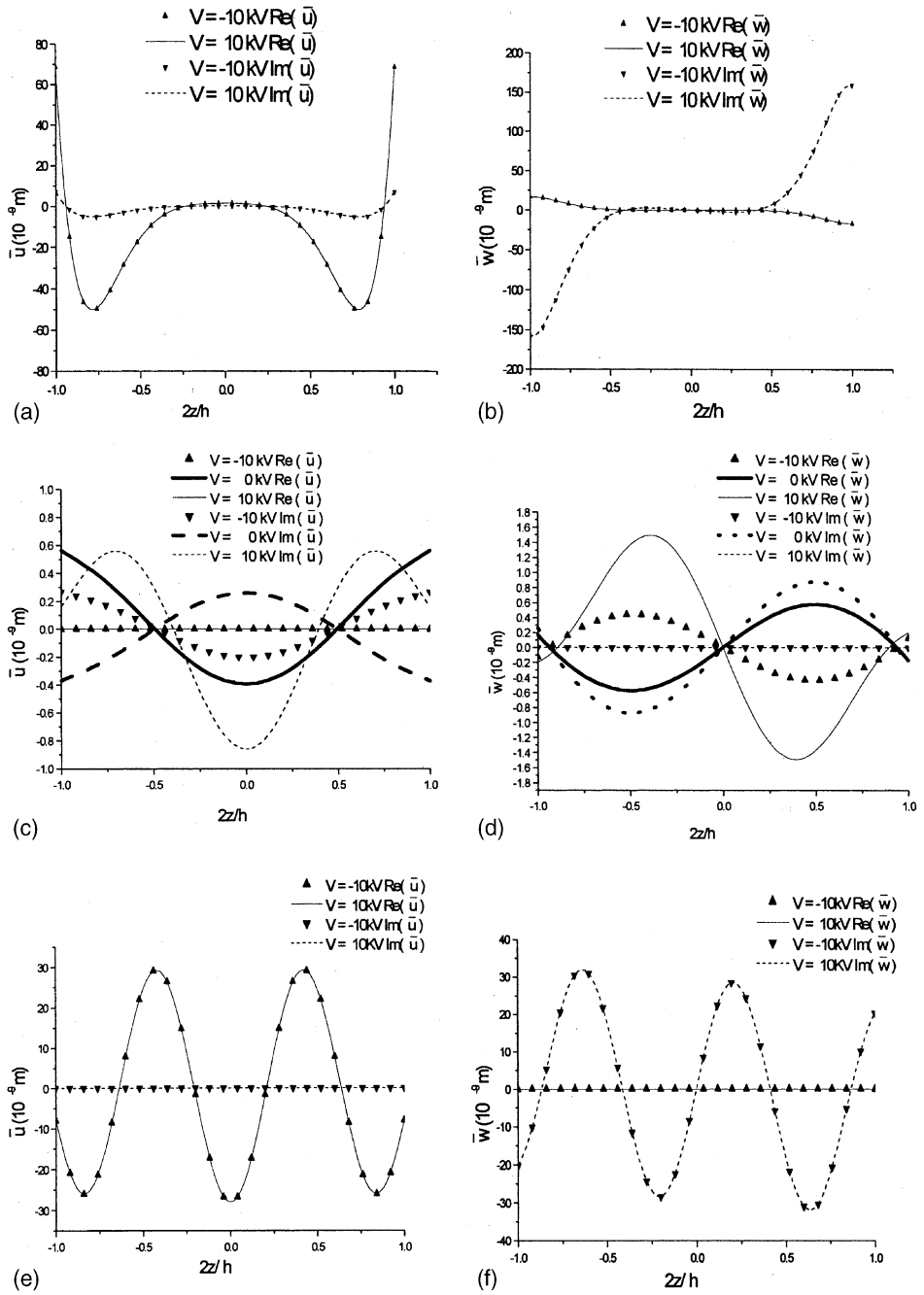

Fig. 5. At $m = 3.0$, variations of particle displacement along thickness of the PZT-5H plate, (a) $\bar{u}$ of s_0 mode, (b) $\overline{w}$ of s_0 mode, (c) $\bar{u}$ of s_1 mode, (d) $\overline{w}$ of s_1 mode, (e) $\bar{u}$ of s_2 mode and (f) $\overline{w}$ of s_2 mode.

fractional change in electromechanical coupling coefficient. It appears that K^2 is maximally increased by 8.728% for the s_2 mode.

4.2. Effect of the biasing electric field on displacements

Variations of the particle displacements of symmetric Lamb modes along the thickness of a PZT-5H plate are plotted in Fig. 5. The horizontal axis is the depth into the material, $2z/h = -1$ corresponds to the top surface of the plate and $2z/h = 1$ bottom surface of the plate. From Fig. 5, it is seen that for $m = 3.0$ (a relative large ratio of plate thickness to wavelength), the biasing electric field has no effect on the displacement components for the s_0 and s_2 modes, and has effects on the s_1 mode. For the s_1 mode, the displacement amplitudes $|u|$ and $|w|$ under unbiased states are always larger than that of the biased states along the plate thickness. For the s_0 mode, a larger fraction of the energy is transported near the two free surfaces. For the higher modes, the curves of displacement component amplitudes are more or less sinusoidal.

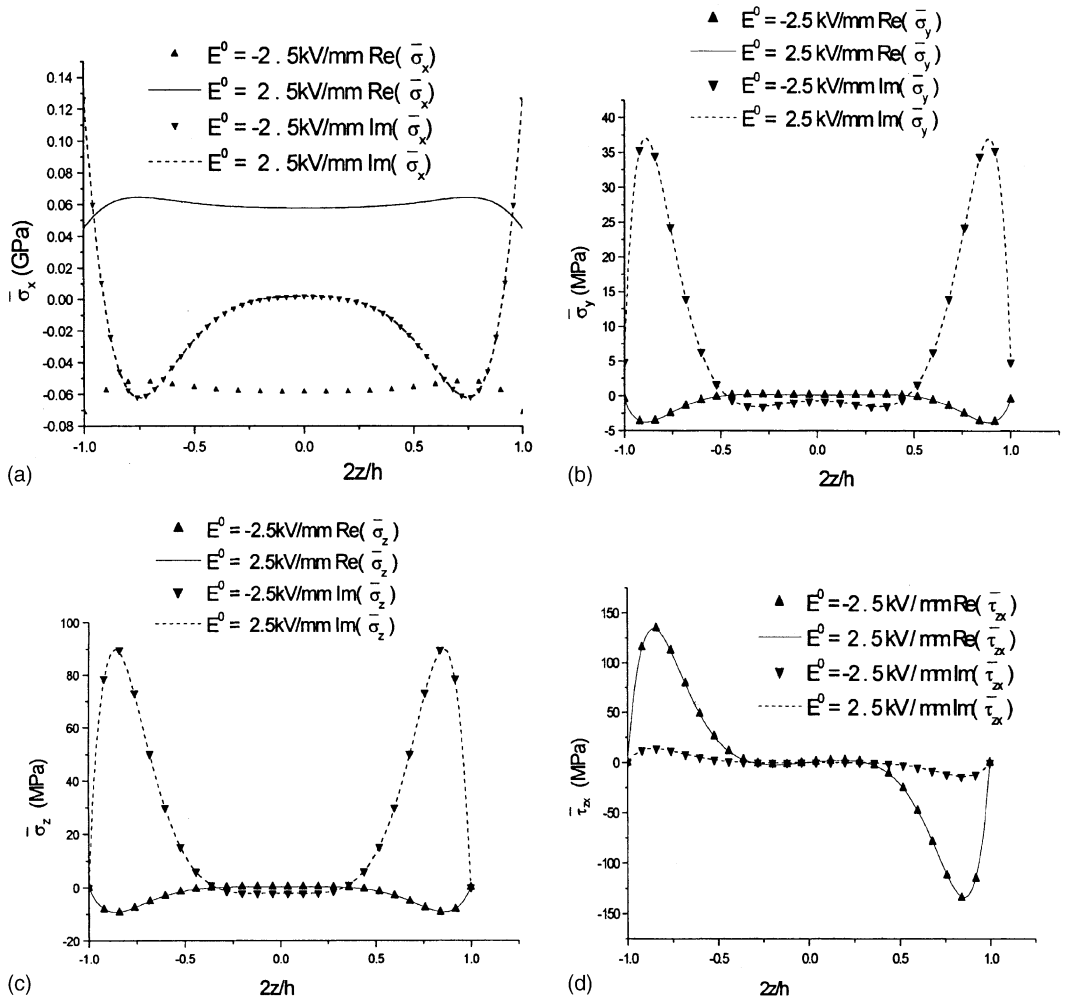

Fig. 6. At $m = 3.0$, variations of stress fields of the s_0 mode along thickness of the PZT-5H plate, (a) $\bar{\sigma}_x$, (b) $\bar{\sigma}_y$, (c) $\bar{\sigma}_z$ and (d) $\bar{\tau}_{zx}$.

4.3. Effect of the biasing electric field on stress fields

For the small-amplitude wave problem superposed on initial stresses, the equations describing the small motion are nonlinear elastic. The Lagrangian stress tensors referred to the reference configuration can be expressed as

$$\sigma_{ij} = \sigma^0_{ij} + \sigma^0_{jr} u'_{i,r} + c_{ijkl} u'_{k,l} + e_{ijn} \varphi'_{,n}$$

where σ_{ij} is the total stress tensor, σ^0_{ij} is initial stress tensor, u'_k and φ' are the component of displacement and electrical potential from the initial equilibrium state to the final state respectively. In this paper, only σ^0_x is considered, so σ_y, σ_z and τ_{zx} have no relation to the initial stress, and only produced by u'_k and φ'. However, for σ_x, we have

$$\sigma_x = \sigma^0_x + \sigma^0_x u'_{1,1} + c_{ijkl} u'_{k,l} + e_{ijn} \varphi'$$

These total stress components of symmetric Lamb wave modes in a biasing electrical field are plotted for $m = 3.0$ in Figs. 6–8. Here, it is seen that σ_x, σ_y and σ_z are symmetric, and τ_{zx} is antisymmetric with respect

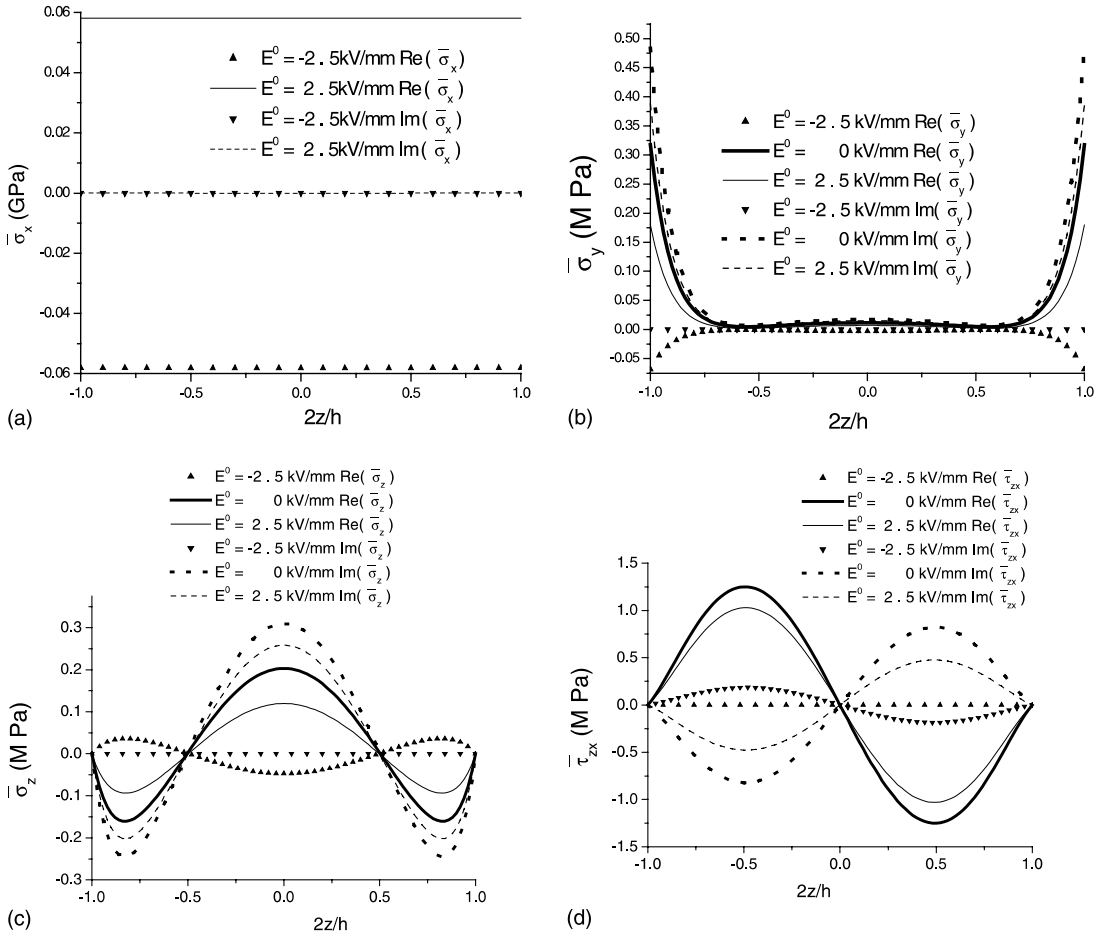

Fig. 7. At $m = 3.0$, variations of stress fields of the s_1 mode along thickness of the PZT-5H plate, (a) $\bar{\sigma}_x$, (b) $\bar{\sigma}_y$, (c) $\bar{\sigma}_z$ and (d) $\bar{\tau}_{zx}$.

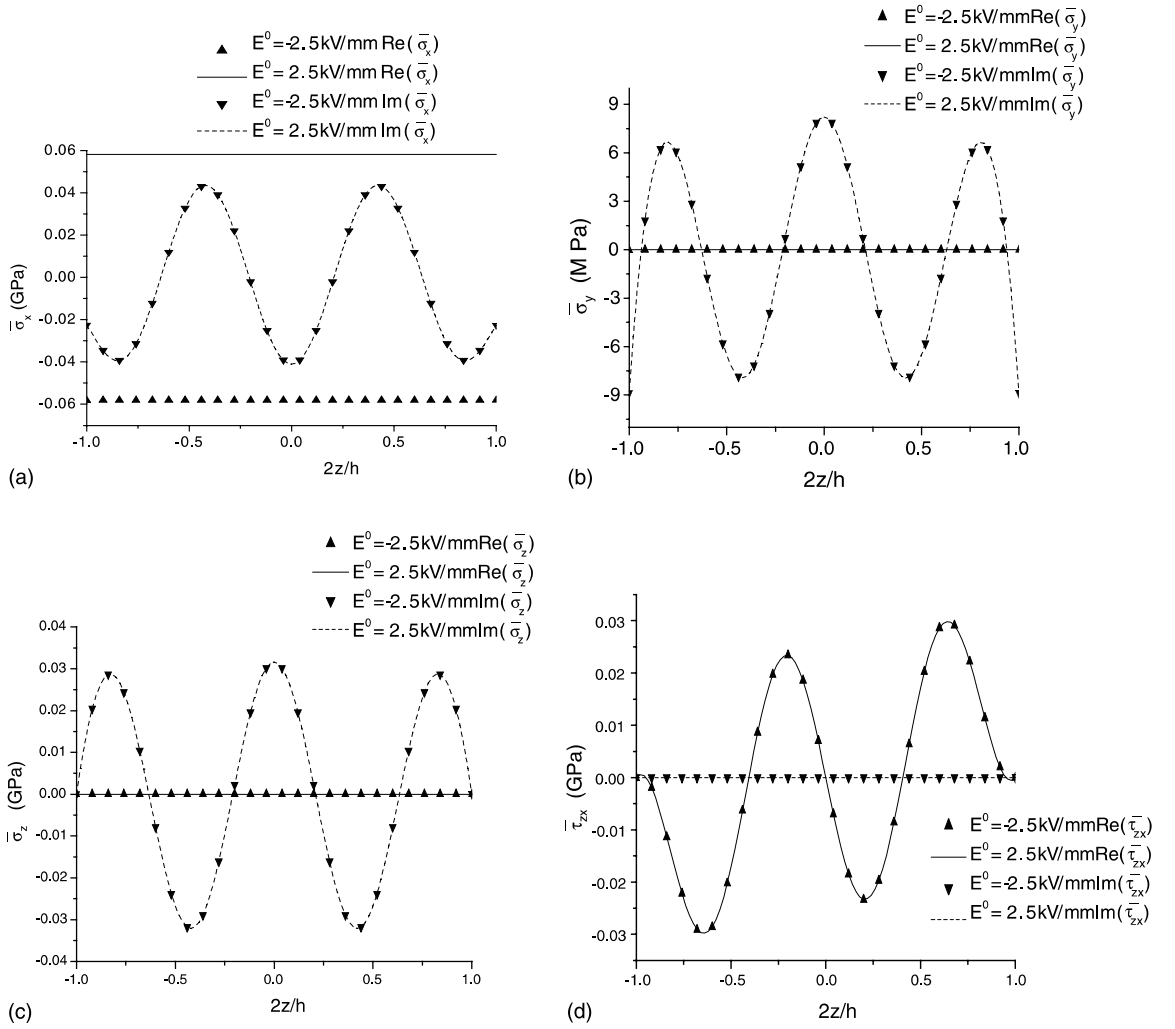

Fig. 8. At $m = 3.0$, variations of stress fields of the s_2 mode along thickness of the PZT-5H plate, (a) $\bar{\sigma}_x$, (b) $\bar{\sigma}_y$, (c) $\bar{\sigma}_z$ and (d) $\bar{\tau}_{zx}$.

to the center plane for symmetric modes. The biasing electric field has no effect on the stress distributions (except σ_x) for the s_0 and s_2 modes. From Fig. 7, for the s_1 mode, it is seen that the stress component σ_y is concentrated near the bottom and top surfaces. For the same value of z, the stress amplitude $|\sigma_y|$ of the unbiased state is larger than that of the biased states. Conversely, other curves of stress component amplitudes are more or less sinusoidal as a function of the plate thickness.

5. Conclusions

The phase velocity, electromechanical coupling coefficient, displacements and stress fields of symmetric Lamb wave modes can be affected by the biasing electric field. The biasing electric field has a significant effect on the phase velocities of Lamb wave modes. For the coordinate system in Fig. 1, the phase velocity

decreases while applying negative biasing voltage and increases while applying positive biasing voltage. For a relative large ratio of plate thickness to wavelength, the maximum fractional velocity change of PZT-5H plates is greater than 0.1% corresponding to a biasing electric field of 2.5 kV/mm. Most experimental works are carried on $LiNbO_3$ crystals. For $LiNbO_3$ crystals (Joshi, 1982; Palma et al., 1985a,b), an electric field of 14 kV/mm can produce fractional time delay changes greater than 0.125%. This indicates that the biasing electric field has a much stronger effect here than in the case of $LiNbO_3$ crystals. The fairly large variation of time delay obtained by the biasing electric field is useful for measurement of high voltages. The determination of high voltages is required in many practical fields such as electrical power systems. The application of these common techniques including electrostatic voltmer, electro-optic voltmer, and acoustic voltmer depends on cost, sensitivity, resolution and so on (Fransen et al., 1997). Lamb wave voltage sensors are sensitive to the biasing electric field. Thus one can accurately measure the changes in time delay to determine the applied voltages. The maximum voltage one can measured is related with the breakdown fields of the material and thickness of the plate. Furthermore, a negative biasing electric field can improve the electromechanical coupling coefficient, one of the most important parameter for the design of piezoelectric devices. But the detailed magnitude can not be calculated according to the change of velocity after metalizing. The biasing electric field has no effect on the displacements for the zero-order mode. However, for large ratios of plate thickness to wavelength, the displacements and stresses of certain higher modes can be affected by a biasing electric field. As a general comment one can state that the use of Lamb modes can lead to a wider choice of improving the characteristics of acoustic devices. Experimental works are still needed to investigate different piezoelectric materials and structures for an enhanced performance.

Acknowledgements

This work is supported by the National Natural Science Foundation through Grants no. 10132010 and 10072033 and the SINO-German Scientific Cooperative Foundation.

References

Dowaikh, M.A., 1999. On SH waves in a pre-stressed layered half-space for an incompressible elastic material. Mech. Res. Commun. 26, 665–672.

Fransen, A., Lubking, G.W., Vellekoop, M.J., 1997. High-resolution high-voltage sensor based on SAW. Sensors Actuat. A 60, 49–53.

Hussain, W., Ogden, R.W., 2001. The effect of pre-strain on the reflection and transmission of plane waves at an elastic interface. Int. J. Engng. Sci. 39, 929–950.

Joshi, S.G., Jin, Y., 1991. Propagation of ultrasonic Lamb waves in piezoelectric plates. J. Appl. Phys. 70, 4113–4120.

Joshi, S.G., 1982. Surface acoustic wave propagation in a biasing electric field. J. Acoust. Soc. Am. 72, 1872–1878.

Joshi, S.G., 1996. Electronically variable time delay in ultrasonic Lamb wave delay lines. IEEE Ultrasonics Symposium, pp. 893–896.

Kessenikh, G.G., Shuvalov, L.A., 1982. Transverse surface waves in piezoelectric crystals of classes 622 and 422. Ferroelectrics 42, 149–152.

Kuznetsova, I.E., Zaitsev, B.D., Polyakov, P.V., Mysenko, M.B., 1998. External electric field effect on the properties of Bleustein-Gulyaev surface acoustic waves in lithium niobate and strontium titanate. Ultrasonics 36, 431–434.

Laurent, T., Bastien, F.O., Pommier, J.C., Cachard, A., Remiens, D., Cattan, E., 2000. Lamb wave and plate mode in ZnO/silicon and AIN/silicon membrane application to sensors able to operate in contact with liquid. Sensors Actuat. A 87, 26–37.

Mesquida, A.A., Otero, J.A., Ramos, R.R., Comas, F., 1998. Wave propagation in layered piezoelectric structures. J. Appl. Phys. 83, 4652–4659.

Palma, A., Palmieri, L., Socino, G., Verona, E., 1985a. Acoustic Lamb wave-electric field nonlinear interaction in YZ $LiNbO_3$ plates. Appl. Phys. Lett. 46, 25–27.

Palma, A., Palmieri, L., Socino, G., Verona, E., 1985b. Lamb-wave electroacoustic voltage sensor. J. Appl. Phys. 58, 3265–3267.

Palmieri, L., Socino, G., Verona, E., 1986. Electroelastic effect in layer acoustic mode propagation along ZnO films on Si substrates. Appl. Phys. Lett. 49, 1581–1583.

Ristic, V.M., 1983. Principles of Acoustic Devices. Wiley, New York, p. 47, 198.
Romos, R.R., Otero, J.A., 1997. Wave propagation in a piezoelectric layer. J. Appl. Phys. 81, 7242–7247.
Shick, D.V., Tiersten, H.F., Sinha, B.K., 1990. Forced thickness-extensional trapped energy vibrations of polarized ceramic plates. J. Appl. Phys. 68, 4998–5008.
Sinha, B.K., 1982. Elastic waves in crystals under a bias. Ferroelectrics 41, 61–73.
Sinha, B.K., Tanski, W.J., Lukaszek, T., Ballato, A., 1985. Influence of biasing stresses on the propagation of surface waves. J. Appl. Phys. 57, 767–776.
Tiersten, T., 1978. Perturbation theory for linear electroelastic equations for small fields superposed on a bias. J. Acoust. Soc. Am. 64, 832–837.
Toda, K., 1973. Lamb-wave delay lines with interdigital electrodes. J. Appl. Phys. 44, 56–62.
Wang, Z.K., Shang, F.L., 1997. Cylindrical buckling of piezoelectric laminated plates. Acta Mechanica Solida Sinica 18, 101–108.
Wenzel, S.W., White, R.M., 1988. Generalized Lamb-wave multisensor. Proceedings of the IEEE Ultrasonics Symposium, pp. 563–567.
Worlton, D.C., 1961. Experimental confirmation of Lamb waves at megacycle frequencies. J. Appl. Phys. 32, 967–972.
Wu, J., Zhu, Z., 1996. Sensitivity of Lamb waves sensors in liquid sensing. IEEE Trans. Ultrason. Ferroelect. Freq. Contr. 43, 71–72.
Xu, Y.X., 1993. Electronic Ceramic Materials. Tian Jin University Press, Tian Jin, China, p. 13.